HST observations of gravitational lens systems *

Emilio E. Falco

Harvard-Smithsonian Center for Astrophysics
Cambridge, MA 02138, USA

CFA-3774

Fermilab Library
0 1160 0035057 3

FERMILAB
NOV 22 1993
LIBRARY

Abstract:
I review the observations of gravitational lens systems and the searches for new systems with the Hubble Space Telescope. Data have been obtained mainly in imaging modes, with the Faint Object Camera and the Wide Field/Planetary Camera. No extended images have been detected (except for the detection of possible giant arcs in the cluster AC114), but several of the "secure" systems with multiply-imaged QSOs were observed. I also discuss briefly the Snapshot Survey, which yielded new interesting statistical results for lensed QSOs.

1 Introduction

The Hubble Space Telescope (HST) has been used to investigate several known gravitational lens systems where the source is a QSO, and also to study the statistics of lensing by means of a survey of bright QSOs.

The Snapshot Survey was a search with HST for new cases of gravitational lensing among QSOs with $M_v < -25.5$, $z > 1$ and $|b| > 10°$, thus tending to maximize the likelihood of lensing for each QSO, and to minimize the contamination of the sample by stars ([BAH92.1]). About 500 QSOs were selected for the survey from the Véron-Cetty and Véron (1991) catalog. The survey yielded a new lens candidate, 1208+1011, and significant new statistical results on the cosmological distribution of gravitational lenses ([MAO93.2], [MAO93.1], [MAO92.1]). The main result of the survey, a lensing frequency between 3 and 6 out of 502 QSOs, could be compared with the predicted frequencies for nonevolving populations of lensing galaxies represented as singular isothermal spheres. In spite of significant remaining uncertainty in the interpretation of the velocity dispersions of the galaxies, the predicted lensing incidence was consistent with the survey measurements, except for strongly λ−dominated cosmologies, which predict unacceptably high values of lensing frequencies. For the sake of brevity, the reader is referred to the suite of Bahcall *et al.* and Maoz *et al.* articles for a clear discussion of the results of the Snapshot Survey.

Although FOC observations of the lens 2237+0305 have been obtained ([CRA91.1]), by far the most popular instrument has been the Wide Field/Planetary Camera (WFPC). The WF and PC are

*Based on observations with the NASA/ESA *Hubble Space Telescope,* obtained at the Space Telescope Science Institute, which is operated by AURA, Inc., under NASA contract NAS 5-26555.

"Gravitational Lenses in the Universe"; 31st Liège Int. Astroph. Coll., 1993

Center for Astrophysics
Preprint Series No. 3717

HST OBSERVATIONS OF GRAVITATIONAL LENS SYSTEMS
Emilio E. Falco

MODELS OF EXTENDED GRAVITATIONAL LENSES
Christopher S. Kochanek

THE THEORETICAL ANALYSIS OF LENS SURVEYS
Christopher S. Kochanek

MAGNIFICATION BIAS AND GRAVITATIONAL LENSING STATISTICS
R. Narayan and S. Wallington

MICROLENSING IN THE TwQSO MIRAGE
Rudy Schild and David J. Thomson

and

MAXIMUM ENTROPY LENS INVERSION
S. Wallington

each a mosaic of four 800 × 800-pixel CCD detectors (labeled WF1–4 and PC5–8, respectively), with angular scales of about 0.1 and 0.04 arcsec per pixel, respectively. Various broadband filters have been used, to wit, F555W (V), F702W (R) and F785LP (R), as detailed below.

In the next two sections, I discuss in some detail two types of observations: GO (general observers) and GTO (guaranteed-time observers). Finally, I discuss briefly the potential for improvement once HST has been refurbished, probably late in 1993.

2 GO observations

The GO observations were obtained by a consortium headed by Ed Turner in a collaboration between Princeton, CfA, MIT, IAS and Caltech. Our targets covered two types of sample: systems thought to be gravitational lenses on the basis of ground-based observations, and several classes of objects that are relatively likely to be undetected gravitational lens systems. In the latter type of sample, we included QSOs with high X-ray luminosity, BL Lac objects, QSOs with high redshift ($z > 4$) and QSOs with high optical luminosity. Our choice of instrument was PC8, which appeared to offer the highest sensitivity of the four PC chips. We selected broad-band filters that approximate the V band (F555W), which should be best for detecting, resolving, and measuring accurate positions of images of lensed (generally relatively blue) QSOs, and the R band (F702W), appropriate for the high redshift QSO sample because the Lyman-alpha absorption forest makes these objects very faint in the F555W band. The results of the observations are summarized in Table 1.

Table 1 shows that the time allotted to each object was divided into a short and a long exposure, to allow us to subtract cosmic ray hits. Each observation was first checked visually to confirm any detection, and promising cases were analyzed further, as detailed below. Out of 27 exposures, two yielded no detection due to a likely underestimation of the magnitudes of the objects, one was a mispointing due to a typographical error in the coordinates provided to STScI, and two were missed, probably due to mispointing by more than the half-width of one PC quadrant.

In the remainder of this section, we analyze in some detail the known lens systems. The astrometry and photometry of images are compared to ground-based measurements. The analysis is carried out mainly on the raw, cosmic-ray subtracted data, with apertures limited to three pixels in radius, to include only the sharp cores of the PSF, to minimize the contamination due to known images and to the much more extended "skirts" of the PSF in each case (see, *e.g.*, [RIX92.1], and Schade and Elson 1993). These sharp cores, which contain about 15% of the light of a well-exposed point source allow one to determine positions and flux ratios of point sources, usually with much greater accuracy than feasible from the ground. A significant contribution of HST to the study of these systems has been a refinement of measurements of the relative positions and of the flux ratios of lensed images (see, *e.g.*, [RIX92.1]).

For some of our observations, it was necessary to perform a deconvolution of the PSF to uncover the complete image morphology. It was found that simple Wiener filtering yielded acceptable results. The deconvolution required a PSF appropriate for the position in the PC where each object was exposed. To calculate such PSFs, we applied software provided by STScI (TinyTim) that takes into account the obscurations and aberration of the telescope. (The PSF varies significantly even over the few arcsec scale characteristic of gravitational lensing.) We also establish limits on the detectability of additional or secondary images, or of lensing galaxies, by constructing simulated images that reproduce the known image morphology, exposure times, filters and PSF (calculated with TinyTim) appropriate for each exposure. The simulations covered densely a wide range of differences in magnitudes, separations, and the full range of azimuth for simulated secondary images and lensing galaxies. We calibrated by estimating the number of counts within a fixed aperture that yielded a definite detection above

the sky and PSF backgrounds; we then compared the counts to the calibration to establish whether detection was feasible in each simulation. Figures 1 through 7 show examples of images corresponding to several of the GO observations, as detailed in the following notes on individual lens systems and QSOs. All the figures are labeled with J2000.0 equatorial coordinates.

2.1 Comments on specific observations

- H 1413+117 : The four known images A, B, C and D ([MAG88.1]) were well detected in V, as shown in Fig. 1 (contours at 50, 25, 12.5, 10, 7.5, 5, 4 and 3% of the peak value) and 2 (contours at 99, 90, 80, 70, 60, 50, 25, 12.5, 10 and 5% of the peak value). Figure 1 shows the raw data, to demonstrate the significant overlap of the extended parts of the PSF in this case; the sharp cores of the PSF are also clearly visible. Figure 2 shows the Wiener-filtered data, with sharper cores, but with significant distributed flux remaining at about the 10% level (compared to the peak, in the southernmost image A). Based on our simulations, we estimate that the undetected lensing galaxy is at least 4 mag fainter than image A. The flux ratios of images B, C and D (corrected for contamination from one another) and of stars 40 and 47 of [KAY90.1] to A are, respectively, 0.85, 0.84, 0.79, 0.69 and 0.13 with uncertainties of about 5% (compare to their ratios, 0.85, 0.74, 0.61, 0.92 and 0.19, respectively). The flux ratios for the images estimated from the Wiener-filtered image agree with the "raw" estimates in the mean to within 5%. The coordinate differences for the QSO cores in our observations agree in the mean with the estimates of these authors to better than 0.02 arcsec; the agreement remains at the same level for the Wiener-filtered images. The very good agreement between the raw and filtered astrometry and photometry is representative for the well-exposed H1413+117, where all images are of very similar brightness, but cannot be expected in cases such as the next one.

- MG 0414+0534 : The four known images A1, A2, B and C ([HEW92.1]) were detected in R, as shown in Fig. 3 (contours at 50, 45, 40, 35, 30, 27 and 25 % of the peak value) and 4 (contours at 50, 45, 40, 35, 30, 27, 25, 23, 21 and 20 % of the peak value). It was difficult to ascertain whether all images were detected based solely on Fig. 3, but Wiener filtering easily revealed the four images ([HEW92.1]), and the possible lensing galaxy that was identified in ground-based observations ([SCH93.1]). The coordinate differences for the images could only be estimated from the Wiener-filtered data; the agreement with and [HEW92.1] was within better than 0.04 arcsec for the brighter images A1, A2 and B, but only 0.2 arcsec for image D, which is very near near the noise level apparent in Fig. 3. The positional disagreement for the possible lens between [SCH93.1] and our observations is about 0.1 arcsec. The flux ratios that we derived for the images of Fig. 4 agree with those of [SCH93.1] to within better than 10%. However, the flux ratios of B and C to the sum of A1 and A2 are larger than those in [HEW92.1] by about a factor of 2. Furthermore, the ratio of the fluxes of A1 and A2 is ~ 0.45 for our data, whereas for the radio data of [HEW92.1] (see their Fig. 1) it is much closer to one. Merging images such as A1 and A2 are expected to have very similar fluxes, thus special conditions must be invoked to rescue the interpretation of the optical observations in a context of gravitational lens models; *e.g.*, obscuration which may be related to the peculiar redness of the spectra of the QSO ([HEW92.1]).

- 0142−100 : The two known images were well detected in V, as shown in Fig. 5 (contours at 80, 50, 25, 12.5, 10, 6, 3.5, 2.5, 1.25 and 0.75 % of the peak value). The brighter image shows the extended skirt of the PSF due to the aberration in the main mirror, but the skirt of the PSF in the fainter image quickly disappears below the noise level. The separation of the images was

2.170 arcsec, with an uncertainty of 0.005 arcsec. in good agreement with the value of 2.22 ± 0.03 of [SUR88.1]. The magnitude difference between the two images was 2.30 ± 0.05 mag, in excellent agreement with the more uncertain estimates of Surdej *et al.*. Based on our simulations, we estimate that the extended lensing galaxy that was clearly apparent in the data of Surdej *et al.* would easily escape detection in our observations in V, assuming only that $V - R \geq 1$ mag. It was found in this case that Wiener-filtering added little new information, mainly because the bright image was well exposed, unlike the faint one, thus the lack of a corresponding figure.

- PKS 0521−365 : The BL Lac was detected at its expected position, see Fig. 6 (contours at 80, 50, 25, 12.5, 6.125, 4 and 3 % of the peak value). The elongation in the lower contours was similarly present in the calculated PSF. Based on the simulations mentioned above, we conclude that secondary images fainter than the primary by 2 (5) mag for separations below 0.1 (above 0.3) arcsec would have been, but were not detected in these exposures.

- PC 1158+4635 : The high-redshift QSO was detected at its expected position, see Fig. 7 (contours at 90, 70, 50, 30, 24 and 18 % of the peak level). The exposure was clearly insufficient to obtain more than a detection of the QSO.

Table 1: 27 observed sources, 1991-1992

Type	Object	Exposure (seconds)	Filter	V (ground) (mag)	Comments
Lens	0023+171	500/1300	F555W	21.5	absent
Lens	0142−100	100/500	F555W	17.0	2 points
Lens	MG0414+0534	500/1000	F702W	24.5	4 points
Lens	MG1131+046	600/1800	F555W	21.5	absent
Lens	1413+117	100/900	F555W	17.0	4 points
Lens	1652+138	500/1000	F555W	20.5	coord. offset
high X	1E1207+3945	200/400	F555W	20.3	1 point
high X	1E2223−0517	200/400	F555W	18.6	missed
BLLac	AO0235+164	140/200	F555W	18.0	1 point
BLLac	B2−1308+326	140/200	F555W	15.2	1 point
BLLac	PKS0521−365	140/200	F555W	14.6	1 point
$z \geq 4$	PC0104+0215	100/350	F702W	20.9	1 point
$z \geq 4$	PC0751+5623	100/350	F702W	21.8	1 point
$z \geq 4$	PC0910+5625	100/350	F702W	22.4	1 point
$z \geq 4$	PC1158+4635	100/350	F702W	22.4	1 point
$z \geq 4$	PC2331+0216	100/350	F702W	21.4	1 point
$z \geq 4$	Q2203+29	100/350	F702W	22.3	1 point
$z \geq 4$	Q0000−26	100/350	F702W	19.0	1 point
$z \geq 4$	Q0046−293	100/350	F702W	20.7	1 point
$z \geq 4$	Q0051−279	100/350	F702W	21.5	1 point
$z \geq 4$	Q0101−304	100/350	F702W	21.0	1 point
high L	Q0159+036	100/350	F555W	16.0	1 point
high L	Q1017+280	100/350	F555W	15.7	1 point
high L	Q1101−264	100/350	F555W	16.0	1 point
high L	Q1623+268B	100/350	F555W	16.0	1 point
high L	Q2127−158	100/350	F555W	16.5	1 point
high L	PG1634+706	100/350	F555W	14.8	1 point

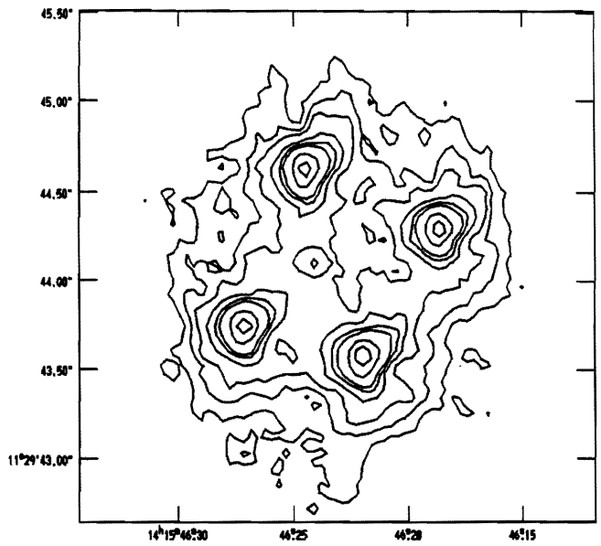

Figure 1: H 1413+117

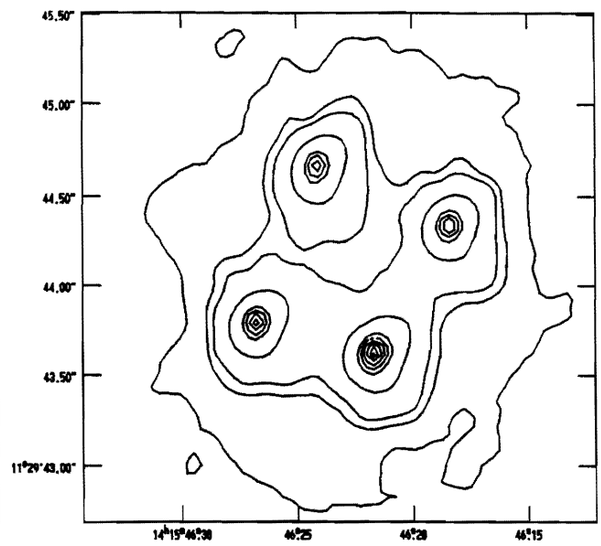

Figure 2: H 1413+117

The last two examples were given to illustrate the bright and the faint ends of our mini-survey for new gravitational lens systems. No new systems were found, not surprisingly, although the relatively short exposures limit the dynamic range for the limits on the presence of faint images that we are able to derive. A detailed analysis of these limits will be published shortly.

3 GTO observations

The archived GTO observations consist of broad-band images acquired with the PC or the WFC of five of the known gravitational lens systems, as shown in Table 2. The filters that were used were F555W and F785LP, with varying exposure times.

In the remainder of this section, I describe qualitatively the results for the three systems that were observed with the PC, that have not been discussed in print, but that are publicly available at the HST archives. I will not describe the FOC and WF observations of Q2237+0305 ([CRA91.1]; [RIX92.1]) or the PC observations of PG1115+080 (Kristian *et al.* 1993, preprint), since these systems were recently described in complete detail in the literature.

3.1 Comments on specific observations

- Q 0957+561 : The two well-known images A (N) and B (S) (*e.g.*, [YOU80.1]) were detected, as well as the main lensing galaxy G1, as shown in Fig. 8 (contours at 50, 25, 5, 3.5 and 2.5 % of the peak level). The observations shown in Fig. 8 and 9 yield the most refined measurements of the coordinate differences between A, B and G1, in good agreement with the VLBI measurements [GOR88.1].

- MG 2016+112 : Two of the known images (A to the NE, and B to the SW, [LAW84.1]) are detected in this case, but are not easily seen in the raw data, which appear to have smaller signal-to-noise ratio than that of Fig. 3. Only the Wiener-filtered R and V exposures are shown

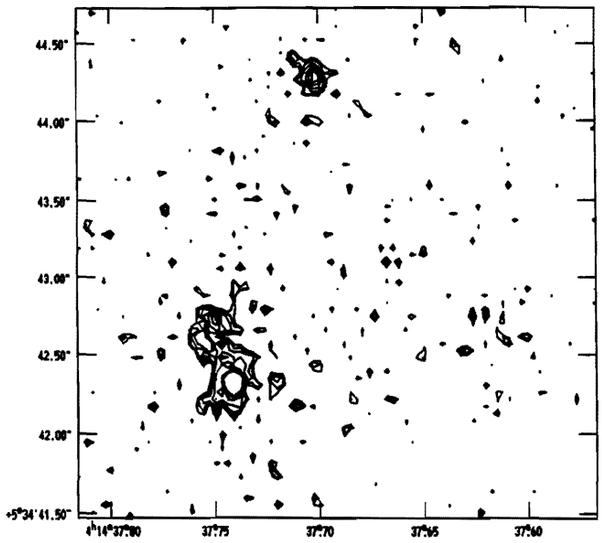

Figure 3: MG 0414+0534

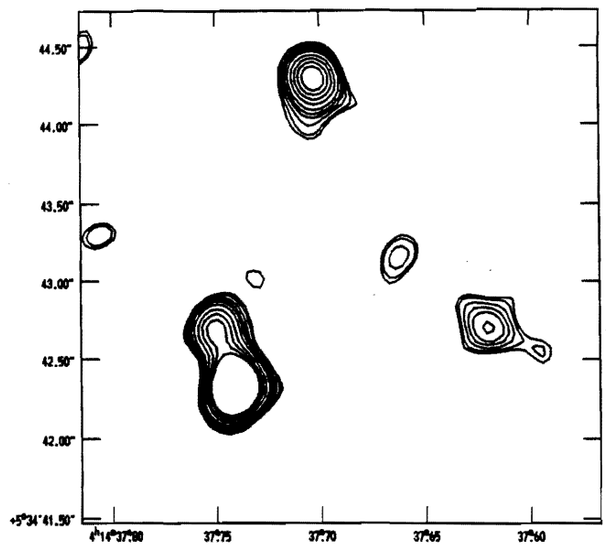

Figure 4: MG 0414+0534

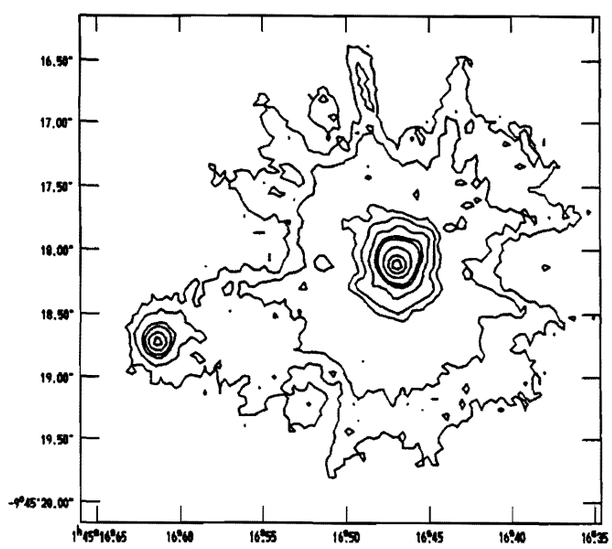

Figure 5: Q 0142−100

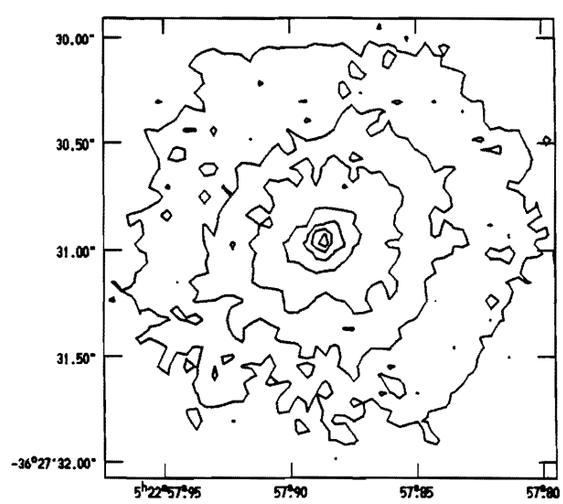

Figure 6: PKS 0521−365

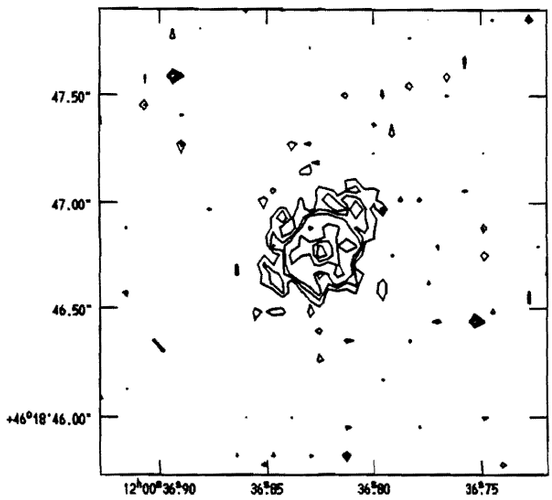

Figure 7: PC 1158+4635

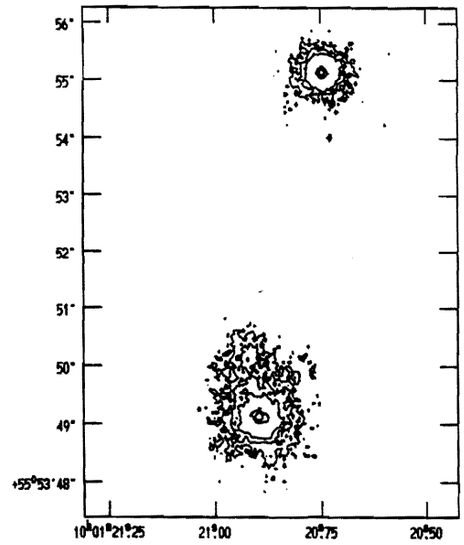

Figure 8: Q 0957+561

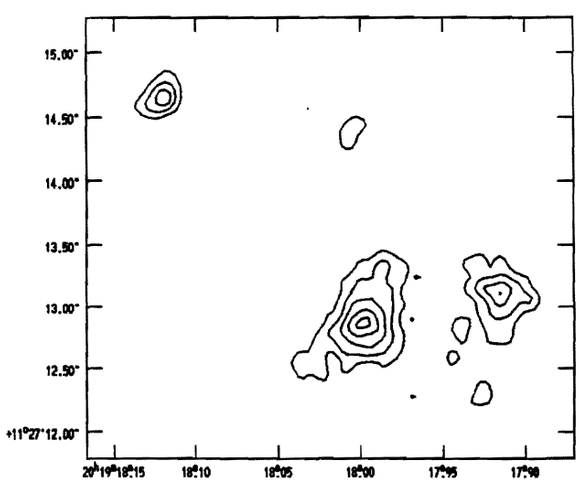

Figure 9: MG 2016+112, R

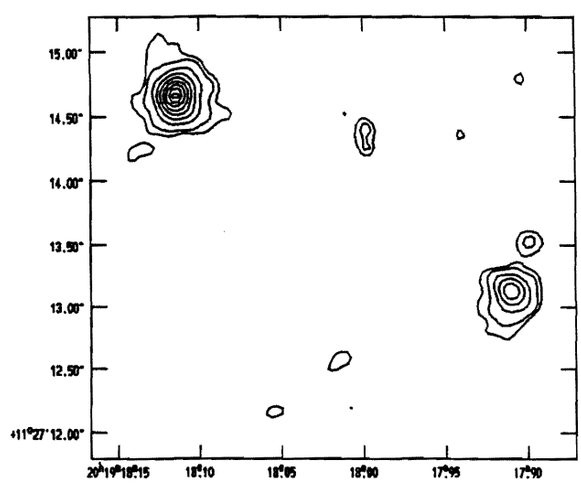

Figure 10: MG 2016+112, V

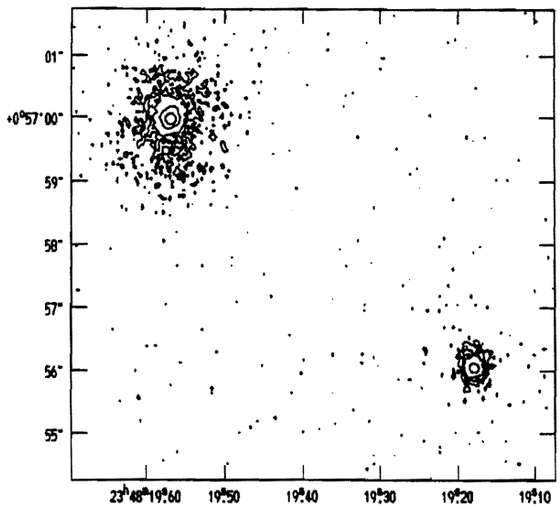

Figure 11: Q 2345+007, R

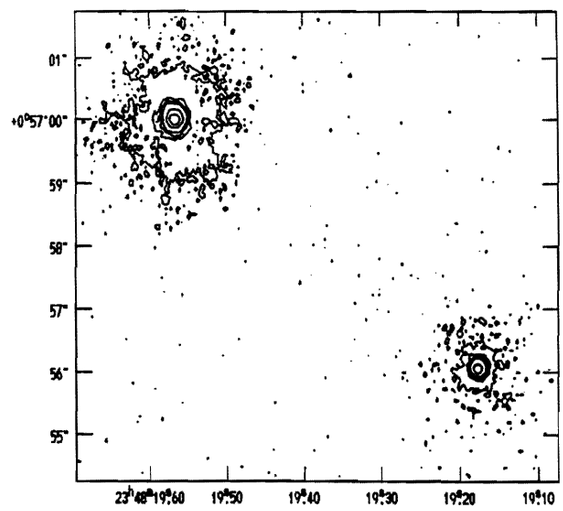

Figure 12: Q 2345+007, V

in Fig. 9 (contours at 99, 95, 90, 85 and 80 % of the peak level) and 10 (contours at 99, 95, 90, 85, 80, 75, 70, 65 and 63 % of the peak level). Images A and B ([LAW84.1]), are seen in both R and V at their expected positions. There is no hint of flux in either band from galaxy C, but galaxy D is clearly visible about 1.2 arcsec E of image B, thus confirming that C is much redder than D, as shown in [LAW93.1].

- Q 2345+007 : The wide-separation QSO images (A to the NE, and B to the SW, [WEE82.1]) were well detected in R and V, respectively, as shown in Fig. 11 (contours at 50, 25, 12.5, 10 and 8 % of the peak level) and 12 (contours at 50, 25, 12.5, 10, 7.5 and 4.5 % of the peak level). The main significance of these two images is that they reveal no doubling of the B image into two components of similar brightness with a separation between 0.3 and 0.4 arcsec, which were reported by Nieto *et al.* [NIE88.1] and by Weir and Djorgovski ([WEI91.1]). Such components are clearly ruled out by these observations. It appears difficult to understand the lack of doubling in 1991 only two years after the observations of Weir and Djorgovski, other than as an instrumental effect in the ground-based observations, thus providing a cautionary note about interpretation of reconstructed images.

Table 2: 5 archive sources

Object	Exposure (seconds)	Filter	V (mag)	z_s	z_d	Images	Max. sep. (arcsec)
Q0957+561	160	F555W	17.4	1.41	0.36	2	6.2
	350	F785LP					
PG1115+080	120	F555W	17.0	1.72	?	4	2.3
	400	F785LP					
MG2016+112	900	F785LP	22.5	3.27	1.01	4?	3.8
Q2237+0305	400	F785LP	16.7	1.695	0.0394	4	1.8
Q2345+007	900	F555W	19.5	2.15	?	2	7.3
	900	F785LP					

4 Future HST observations

The scheduled repair mission of HST holds the promise of restoring the full capability of the telescope. Very significant improvements are expected for photometry, astrometry and spectroscopy. In the upcoming cycle 4, post-repairs, we expect to reobserve most of our GO targets with WFPC2, and with much longer exposures. Thus, we should be able to detect the missing lenses, or to set very deep limits on their fluxes, especially in the cases of the two ring systems. These measurements will constrain model parameters that will be used in the further analysis of future ground-based observations, in particular those aimed at obtaining estimates of the time delays for several lens systems, to continue a search for new estimates of the Hubble constant. Thus, the potential of HST for studies of gravitational lenses remains to be realized fully. We remain optimistic.

Acknowledgements

I gratefully acknowledge the support of STScI grant GO-2350.02-87A.

References

Schade, D. J. and Elson, R. A. W. 1993, *A. J.*, **105**, 1581

Véron-Cetty, M. P. and Véron, P. 1991, "A Catalogue of Quasars and Active Nuclei" (5th ed.; Munich: ESO)